Nonconservative dipole forces on an excited two-atom system

J. Sánchez-Cánovas and M. Donaire*

Departamento de Física Teórica, Atómica y Óptica and IMUVA, Universidad de Valladolid, Paseo Belén 7, 47011 Valladolid, Spain

(Received 29 November 2021; revised 30 May 2022; accepted 25 August 2022; published 8 September 2022)

We compute the nonconservative electric dipole forces between the atoms of a suddenly excited binary system. These forces derive from the time variation of the longitudinal electromagnetic momentum. In contrast to the conservative van der Waals forces, the nonconservative forces possess components orthogonal to the interatomic axis. Thus, despite being several orders of magnitude smaller than van der Waals', they might be accessible experimentally. For the case of a binary system of identical atoms in Dicke states, these forces are reciprocal. However, when only one of the atoms is initially excited, as with the van der Waals forces, the nonconservative ones are nonreciprocal, which results in a net force on the two-atom system. We offer an estimate of the spatial displacement caused by the nonconservative forces on a binary system of hydrogen atoms.

DOI: 10.1103/PhysRevA.106.032805

I. INTRODUCTION

Nonconservative forces are usually identified with velocity-dependent forces and with dissipative forces mediated by incoherent processes. As for the former, common examples are the Lorentz magnetic force and friction forces generated by the relative motion between charged bodies—e.g., magnetic friction and quantum friction forces [1–3]. As for the latter, nonconservative forces involve the coupling of the system under study to a reservoir. In this respect, several proposals have been made to employ nonconservative dissipative forces to bind, to pair, and to stabilize the constituents of quantum systems [4–6].

The present paper deals with nonconservative fundamental forces instead. Thus, we show that nonconservative forces are exerted upon the constituents of a dynamical quantum system whose internal interactions are mediated by gauge fields. In particular, we prove this on a binary system of excited atoms. In brief, the existence of fundamental nonconservative forces has its origin in the difference between the canonical conjugate momentum and the kinetic momentum. That is, in quantum field theory a gauge interaction is incorporated through the so-called *minimal coupling*, which consists of the replacement of the ordinary derivative with the covariant derivative in the free Lagrangian of the charged fields. Ordinary and covariant derivatives differ in a term linear in the gauge field and the coupling constant. Mathematically, the gauge field is the connection of the fiber bundle associated with the group of the gauge symmetry. Physically, that implies the replacement of the four-canonical momentum with four-energy-kinetic momentum vector of the charged particles [7,8]. Hence, the difference between both momenta is a gauge field term which, for the case of the electromagnetic interaction, is referred to as longitudinal electromagnetic momentum [9]. Note that the representation of the three-canonical momentum in the position basis of quantum mechanics is the ordinary gradient operator which, incidentally, enters the expression of the conservative forces as the gradient of a scalar potential. However, the total force operator is the time derivative of the kinetic momentum operator. Hence, as we will show later, it is the time derivative of the difference between the canonical momentum and the kinetic momentum, i.e., of the longitudinal momentum in the electromagnetic case, the one to be identified with (fundamental) nonconservative forces. We emphasize that, in contrast to the aforementioned nonconservative forces, the fundamental ones do not depend on kinematics or effective dissipative effects. For simplicity, we have computed these forces on an excited atomic system, but analogous nonconservative forces are to be found, for instance, in nuclear systems whose weak interaction is mediated by $W^{\pm}$ and Z bosons. Nonetheless, in the remainder of this article we restrict ourselves to the electromagnetic forces of atomic systems.

Dispersion forces between neutral atoms in the electric dipole approximation are generally referred to as van der Waals (vdW) forces [10–17]. They are the result of the coupling of the quantum fluctuations of the electromagnetic (EM) field in its vacuum state with the dipole fluctuations of the atomic charges in stable or metastable states. For a system of atoms in their ground states the vdW forces can be computed applying the usual techniques of stationary quantum perturbation theory. Those forces are conservative and reciprocal and can be expressed in terms of the atomic polarizabilities [12–17]. In contrast, when atoms are excited, it has been proven in Refs. [18–26] that a fully stationary treatment is insufficient to account for the incoherent dynamics of a metastable system. In particular, for a system of two dissimilar atoms with one of them initially excited, the time-dependent approaches of Refs. [19,22,26], in the adiabatic limit, have shown that whereas the resonant component of the vdW force upon the excited atom oscillates in space, the resonant force on the de-excited atom decreases monotonically with the interatomic distance. The nonreciprocity of the vdW forces

*manuel.donaire@uva.es

results in an apparent violation of the classical action-reaction principle and the conservation of total momentum, which would be in contradiction with the invariance of the system under global spatial translation. This apparent contradiction was solved in Ref. [27] where it was shown that the *missing* momentum was carried by the photons which mediate the interaction which, ultimately, causes the directionality of spontaneous emission when the system gets deexcited. The vdW forces between dissimilar atoms either resonant or off-resonant are all quasistationary for an adiabatic excitation and can be expressed in terms of the gradients of the expectation values of the interaction potentials [26,27], hence, reflecting their conservative nature.

As for the case of a binary system of identical atoms, with one of them initially excited, it has been shown in Ref. [28] that the vdW forces are inherently time dependent and grow linearly with time in the weak-interaction regime. This is so because, on the one hand, the system is degenerate, and an adiabatic excitation is not feasible. In fact, a sudden excitation is generally a good approximation to model the preparation of the initial state of the system. On the other hand, that excited state is highly nonstationary since its dynamics comprises both the coherent transfer of the excitation between the atoms and its incoherent decay through spontaneous emission.

Besides, it was found in Ref. [28] that, still in the electric dipole approximation, when the atomic interaction depends on time, in addition to the conservative vdW forces, nonconservative forces arise from the time variation of the aforementioned EM longitudinal momentum, which can be expressed, in general, in terms of the EM vector potential or in terms of electric and magnetic fields [9,29–33]. Since the interaction between two atoms becomes time dependent when one of them is excited nonadiabatically, so does the EM longitudinal momentum of the system. Thus, nonconservative forces arise in a binary system if excited nonadiabatically and, as for the case of the conservative vdW forces, their strength is greater for the case of identical atoms.

In this article we aim at computing the nonconservative forces on a binary system of two-level atoms, paying special attention to the case of identical atoms. We will show that they contain components orthogonal to the interatomic axis which might be accessible experimentally. We will estimate the spatial displacement caused by the nonconservative dipole forces on a binary system of hydrogen atoms. In addition, as for the case of conservative vdW forces when the system is asymmetrically excited, say, for instance, when only one of the atoms is initially excited, we will show that nonconservative forces are nonreciprocal, which results in a net nonconservative force upon the two-atom system—see Fig. 1.

The article is organized as follows. In Sec. II we explain the formalism of our Hamiltonian approach. In Sec. III we perform the computation of the nonconservative forces between two dissimilar two-level atoms, one of which is suddenly excited. The identical atoms limit is considered in Sec. IV in the weak-interaction regime. The case of Dicke states is addressed too. In Sec. V we estimate the displacement caused on an excited binary system of hydrogen atoms by the orthogonal components of the nonconservative forces. The conclusions are summarized in Sec. VI together with a discussion.

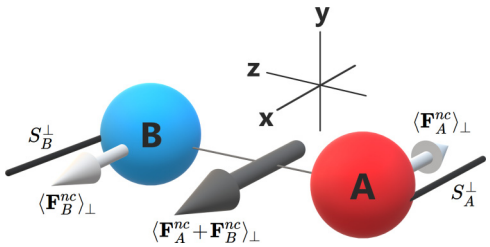

FIG. 1. Pictorial representation of the action of the orthogonal components of the nonconservative forces upon a binary atomic system $\langle \mathbf{F}_{A,B}^{nc} \rangle_\perp$, which cause the displacements of the atoms in a direction orthogonal to the interatomic axis $S_{A,B}^\perp$. For an asymmetrically excited system, a net force emerges $\langle \mathbf{F}_A^{nc} + \mathbf{F}_B^{nc} \rangle_\perp$.

II. FUNDAMENTALS OF THE APPROACH

Let us take a system of two two-level atoms A and B, located a distance R apart. In the first place, let us consider dissimilar atoms with resonance frequencies ω_A and ω_B, detuning $\Delta_{AB} = \omega_A - \omega_B$, natural linewidths Γ_A and Γ_B with the excited level of atom B being n-fold degenerate. Since we are ultimately interested in the identical atoms limit, $|\Delta_{AB}| \ll \Gamma_A$, $\Gamma_A \to \Gamma_B$, atoms are assumed to be suddenly excited with an external field of strength $\Omega \gg |\Delta_{AB}|$. Thus, when only one of the atoms is excited, say atom A, the state of the system at time 0 will be $|\Psi(0)\rangle = |A_+\rangle \otimes |B_-\rangle \otimes |0_\gamma\rangle$, where $|A_+\rangle$ is the excited state of atom A, $|(A,B)_-\rangle$ denote the ground states of the atoms A and B, respectively, $|0_\gamma\rangle$ is the EM vacuum state, and the states of the n-fold degenerate excited state of atom B will be denoted by $\{|b\rangle\}$. When the excitation is delocalized between the two atoms we will restrict ourselves to the symmetric $(+)$ and antisymmetric $(-)$ Dicke states, in which case $|\Psi(0)\rangle$ takes the form $|\Psi_\pm(0)\rangle = [|A_+\rangle \otimes |B_-\rangle \pm |A_-\rangle \otimes |B_+\rangle] \otimes |0_\gamma\rangle/\sqrt{2}$, respectively. At time $T > 0$ the state of the two-atom-EM field system reads $|\Psi(T)\rangle = \mathbb{U}(T)|\Psi(0)\rangle$, where $\mathbb{U}(T)$ denotes the time propagator in the Schrödinger representation,

$$\mathbb{U}(T) = \mathcal{T} - \exp\left\{-i\hbar^{-1}\int_0^T dt\, H\right\},$$
$$H = \mathcal{T} + H_A + H_B + H_{EM} + W. \tag{1}$$

In this equation $\mathcal{T} = m_A|\dot{\mathbf{R}}_A|^2/2 + m_B|\dot{\mathbf{R}}_B|^2/2$ is the kinetic energy of the center of mass of the atomic system with $m_{A,B}$ being the atomic masses and $\mathbf{R}_{A,B}$ being the position vectors of the centers of mass of each atom. $H_A + H_B$ is the free Hamiltonian of the internal atomic states, $\hbar\omega_A|A_+\rangle\langle A_+| + \sum_b \hbar\omega_B|b\rangle\langle b|$, and the Hamiltonian of the free EM field is $H_{\rm EM} = \sum_{\mathbf{k},p} \hbar\omega(a_{\mathbf{k},p}^\dagger a_{\mathbf{k},p} + 1/2)$, where $\omega = ck$ is the photon frequency, and the operators $a_{\mathbf{k},p}^\dagger$ and $a_{\mathbf{k},p}$ are the creation and annihilation operators of photons with momentum $\hbar\mathbf{k}$ and polarization index p, respectively. Finally, the interaction Hamiltonian in the electric dipole approximation reads $W = W_A + W_B$ with

$$W_{A,B} \approx -\mathbf{d}_{A,B} \cdot \mathbf{E}(\mathbf{R}_{A,B}). \tag{2}$$

In this equation the electric dipole operators are denoted by $\mathbf{d}_{A,B}$, and $\mathbf{E}(\mathbf{R}_{A,B})$ and $\mathbf{B}(\mathbf{R}_{A,B})$ are the quantum electric and magnetic-field operators in Schrödinger's

representation, respectively. In terms of the EM vector potential, in the Coulomb gauge $\nabla \cdot \mathbf{A}(\mathbf{r},t)=0$, the electric- and magnetic-fields $\mathbf{E}(\mathbf{R}_{A,B})=-\partial_t \mathbf{A}(\mathbf{R}_{A,B},t)|_{t=0}$, $\mathbf{B}(\mathbf{R}_{A,B})=\nabla_{A,B}\wedge\mathbf{A}(\mathbf{R}_{A,B})|_{t=0}$ can be written as sums over normal modes as [12,16]

$$\begin{aligned}\mathbf{E}(\mathbf{R}_{A,B}) &= \sum_{\mathbf{k}}[\mathbf{E}^{(-)}_{\mathbf{k}}(\mathbf{R}_{A,B})+\mathbf{E}^{(+)}_{\mathbf{k}}(\mathbf{R}_{A,B})]\\ &= i\sum_{\mathbf{k},p}\sqrt{\frac{\hbar ck}{2\mathcal{V}\epsilon_0}}[\boldsymbol{\epsilon}_p a_{\mathbf{k},p}e^{i\mathbf{k}\cdot\mathbf{R}_{A,B}}-\boldsymbol{\epsilon}^*_p a^\dagger_{\mathbf{k},p}e^{-i\mathbf{k}\cdot\mathbf{R}_{A,B}}],\\ \mathbf{B}(\mathbf{R}_{A,B}) &= \sum_{\mathbf{k}}[\mathbf{B}^{(-)}_{\mathbf{k}}(\mathbf{R}_{A,B})+\mathbf{B}^{(+)}_{\mathbf{k}}(\mathbf{R}_{A,B})]\\ &= i\sum_{\mathbf{k},p}\sqrt{\frac{\hbar}{2ck\mathcal{V}\epsilon_0}}\\ &\quad\times\mathbf{k}\wedge[\boldsymbol{\epsilon}_p a_{\mathbf{k},p}e^{i\mathbf{k}\cdot\mathbf{R}_{A,B}}-\boldsymbol{\epsilon}^*_p a^\dagger_{\mathbf{k},p}e^{-i\mathbf{k}\cdot\mathbf{R}_{A,B}}],\end{aligned}$$

where $\mathcal{V}$ is a generic volume and $\mathbf{E}^{(\mp)}_{\mathbf{k}}$, $\mathbf{B}^{(\mp)}_{\mathbf{k}}$ denote the annihilation and creation electric- and magnetic-field operators of photons of momentum $\hbar\mathbf{k}$ and polarization vector $\boldsymbol{\epsilon}_p$, respectively. Strictly speaking, W includes and additional term in the electric dipole approximation which is referred to as a Röntgen term [32,33]. As argued in Ref. [3], that term is negligible since its contribution to Eq. (1) contains terms of orders $\dot{R}_{A,B}/c$ and $\mathbf{d}_{A,B}\cdot\mathbf{E}(\mathbf{R}_{A,B})/m_{A,B}$ smaller than the contributions of that in Eq. (2) with $m_{A,B}$ being the atomic masses [34]. Next, considering W as a perturbation to the free Hamiltonians, the unperturbed time propagator for atom and free photon states is $\mathbb{U}_0(t)=\exp[-i\hbar^{-1}(\mathcal{T}+H_A+H_B+H_{\mathrm{EM}})t]$. In terms of W and $\mathbb{U}_0$, $\mathbb{U}(T)$ admits an expansion in powers of W which can be developed out of its time-ordered exponential expression,

$$\mathbb{U}(T)=\mathbb{U}_0(T)T-\exp\int_0^T(-i/\hbar)\mathbb{U}_0^\dagger(t)W\mathbb{U}_0(t)dt, \quad (3)$$

which can be written as $\mathbb{U}(T)=\mathbb{U}_0(T)+\sum_{n=1}^{\infty}\delta\mathbb{U}^{(n)}(T)$ with $\delta\mathbb{U}^{(n)}$ being the term of order W^n. The system possesses a conserved total momentum, $\mathbf{K}=\mathbf{P}_A+\mathbf{P}_B+\mathbf{P}^\gamma_\perp$—with $\mathbf{P}_{A,B}$ and $\mathbf{P}^\gamma_\perp=\sum_{\mathbf{k},p}\hbar\mathbf{k}\,a^\dagger_{\mathbf{k},p}a_{\mathbf{k},p}$ being the canonical conjugate momentum of each atom and the transverse EM momentum, respectively, which satisfies $[H,\mathbf{K}]=\mathbf{0}$ [9,29,31]. Furthermore, if the charges $\{q_i\}$ within the atoms are considered individually at positions $\{\mathbf{r}_i\}$, the total canonical conjugate momentum can be written as

$$\mathbf{P}_A+\mathbf{P}_B=m_A\dot{\mathbf{R}}_A+m_B\dot{\mathbf{R}}_B+\sum_i q_i\mathbf{A}(\mathbf{r}_i), \quad (4)$$

where the first two terms are the kinetic momenta of the centers of mass of each atom. As for the momentum within the summation symbol, once the Coulomb gauge is taken and $\mathbf{A}(\mathbf{r})$ becomes fully transverse $\mathbf{A}(\mathbf{r})=\mathbf{A}_\perp(\mathbf{r})$, it corresponds to the longitudinal EM momentum [9,29] $\mathbf{P}^\gamma_\parallel=\sum_i q_i\mathbf{A}_\perp(\mathbf{r}_i)$, which is manifestly gauge invariant. Hence, it can be written in terms of the Coulomb electric field and the magnetic field generated by the internal motion of the atomic charges, $\mathbf{P}^\gamma_\parallel=\int d^3\mathbf{r}\;\mathbf{E}_{\mathrm{Coul}}(r)\wedge\mathbf{B}(r)$ [9,35]. Furthermore, a multipole expansion allows to express $\mathbf{P}^\gamma_\parallel$ in the electric dipole approximation as [32,33]

$$\mathbf{P}^\gamma_\parallel\simeq-\mathbf{d}_A\wedge\mathbf{B}(\mathbf{R}_A)-\mathbf{d}_B\wedge\mathbf{B}(\mathbf{R}_B). \quad (5)$$

Following Refs. [3,27], the electric dipole force on each atom is computed applying the time derivative to the expectation value of the kinetic momenta of the centers of mass of each atom. Writing the latter in terms of the canonical conjugate momenta and the longitudinal EM momentum, in the electric dipole approximation, we arrive at

$$\begin{aligned}\langle\mathbf{F}_{A,B}\rangle &= \partial_T\langle m_{A,B}\dot{\mathbf{R}}_{A,B}\rangle\\ &= -i\hbar\partial_T\langle\Psi(0)|\mathbb{U}^\dagger(T)\nabla_{A,B}\mathbb{U}(T)|\Psi(0)\rangle\\ &\quad+\partial_T\langle\Psi(0)|\mathbb{U}^\dagger(T)\mathbf{d}_{A,B}\wedge\mathbf{B}(\mathbf{R}_{A,B})\mathbb{U}(T)|\Psi(0)\rangle\\ &= -\langle\nabla_{A,B}W_{A,B}\rangle+\partial_T\langle\mathbf{d}_{A,B}\wedge\mathbf{B}(\mathbf{R}_{A,B})\rangle. \quad (6)\end{aligned}$$

The first term on the right-hand side of the last equality corresponds to the conservative vdW forces along the interatomic axis, already computed in Ref. [28]. As advanced in the Introduction, the second term corresponds to the nonconservative forces we are interested in $\langle\mathbf{F}^{nc}_{A,B}\rangle=\partial_T\langle\mathbf{d}_{A,B}\wedge\mathbf{B}(\mathbf{R}_{A,B})\rangle$, which equal the time derivatives of the components of the

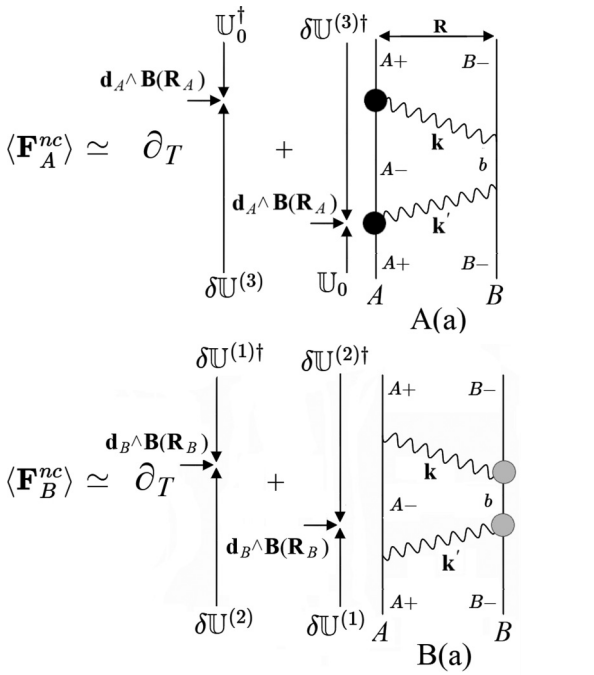

FIG. 2. Diagrammatic representation of the dominant processes which contribute to A(a) $\langle\mathbf{F}^{nc}_{A,B}\rangle$ and B(a) $\langle\mathbf{F}^{nc}_{A,B}\rangle$. Solid straight lines stand for propagators of atomic states, whereas wavy lines stand for photon propagators. Atomic and photon states are indicated explicitly. The atoms A and B are separated by a distance R along the horizontal direction, whereas time runs along the vertical. The big circles in black and gray stand for the insertion of the Schrödinger operators $\mathbf{d}_{A,B}\wedge\mathbf{B}(\mathbf{R}_{A,B})$, respectively, whose expectation values are computed. Each diagram contributes with two terms, one from each of the operators inserted. They are sandwiched between two time propagators, $\mathbb{U}(T)$ and $\mathbb{U}^\dagger(T)$ (depicted by vertical arrows), which evolve the initial-state $|\Psi(0)\rangle$ towards the observation time at which $\mathbf{d}_{A,B}\wedge\mathbf{B}(\mathbf{R}_{A,B})$ apply.

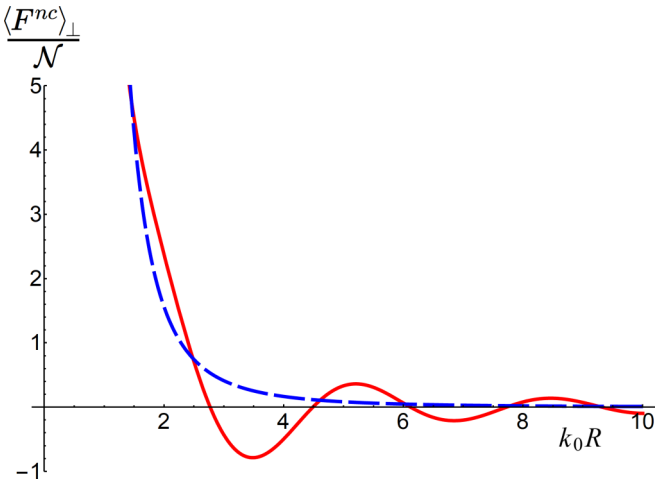

FIG. 3. Graphical representation of the spatial behavior of the nonconservative forces in the identical-atom limit according to Eq. (10). The solid line in red represents $\mathrm{Tr}\{\langle \mathbf{F}_A^{nc}\rangle \cdot \alpha\}$, whereas the dashed line in blue is for $\mathrm{Tr}\{\langle \mathbf{F}_B^{nc}\rangle \cdot \alpha\}$. Both curves are normalized to $\mathcal{N} = \frac{k_0^6|\boldsymbol{\mu}|^4(1-\Gamma_0 T)e^{-\Gamma_0 T}}{80\pi^2\epsilon_0^2\hbar c}$, and transition dipole moments are considered isotropic.

longitudinal EM momentum with opposite signs. It is worth noting at this point that nonconservative forces associated to the time variation of the longitudinal EM momentum have been already found in chiral systems subject to the adiabatic increasing of a uniform magnetic field [35,36].

III. NONCONSERVATIVE FORCES ON A BINARY SYSTEM OF DISSIMILAR ATOMS

As explained in the previous section, let us consider that one of the atoms, say A, is excited suddenly at the initial time. A perturbative development of Eq. (6) shows that, up to terms involving two-photon exchange processes, 12 diagrams contribute to $\langle \mathbf{F}_A^{nc}\rangle$ and $\langle \mathbf{F}_B^{nc}\rangle$ for the interaction between two-level atoms. These are depicted diagrammatically in Fig. 7 in Appendix A. The contributions of each process to $\langle \mathbf{F}_A^{nc}\rangle$ and $\langle \mathbf{F}_B^{nc}\rangle$ are analogous to those of the vdW forces computed in Ref. [28], but for the replacement of the operators $-\boldsymbol{\nabla}_{A,B}W_{A,B}$ with $\partial_T \mathbf{d}_{A,B} \wedge \mathbf{B}(\mathbf{R}_{A,B})$ acting upon one of the exchanged photons.

For $|\Delta_{AB}| \ll \omega_{A,B}$, diagrams A(a) and B(a) of Fig. 2 render the leading contribution to the forces. In Appendix A we illustrate their calculation with the detailed reading of the contribution of diagram A(a) to $\langle \mathbf{F}_A^{nc}\rangle$. Operating in an analogous fashion with the term derived from the diagram B(a) for $\langle \mathbf{F}_B^{nc}\rangle$, upon integration in the momenta of the virtual photons k and k' in the complex plane, we arrive at (see Fig. 3).

$$\begin{aligned}\langle \mathbf{F}_A^{nc}\rangle \simeq \sum_b \Bigg\{ & \frac{2\omega_A^3\Gamma_A e^{-\Gamma_A T}}{c^4\epsilon_0^2\hbar\Delta_{AB}}[\boldsymbol{\mu}_A \wedge \boldsymbol{\nabla} \wedge \mathrm{Re}\,\mathbb{G}(k_A R)\cdot\boldsymbol{\mu}_b\boldsymbol{\mu}_b\cdot \mathrm{Im}\,\mathbb{G}(k_A R)\cdot\boldsymbol{\mu}_A + \boldsymbol{\mu}_A \wedge \boldsymbol{\nabla} \wedge \mathrm{Im}\,\mathbb{G}(k_A R)\cdot\boldsymbol{\mu}_b\boldsymbol{\mu}_b\cdot \mathrm{Re}\,\mathbb{G}(k_A R)\cdot\boldsymbol{\mu}_A] \\ & - \frac{\omega_B^3 e^{-(\Gamma_A+\Gamma_b)T/2}}{c^4\epsilon_0^2\hbar}\left[2\sin(\Delta_{AB}T) + \frac{\Gamma_A+\Gamma_b}{\Delta_{AB}}\cos(\Delta_{AB}T)\right][\boldsymbol{\mu}_A \wedge \boldsymbol{\nabla} \wedge \mathrm{Re}\,\mathbb{G}(k_B R)\cdot\boldsymbol{\mu}_b\boldsymbol{\mu}_b\cdot \mathrm{Im}\,\mathbb{G}(k_B R)\cdot\boldsymbol{\mu}_A \\ & + \boldsymbol{\mu}_A \wedge \boldsymbol{\nabla} \wedge \mathrm{Im}\,\mathbb{G}(k_B R)\cdot\boldsymbol{\mu}_b\boldsymbol{\mu}_b\cdot \mathrm{Re}\,\mathbb{G}(k_B R)\cdot\boldsymbol{\mu}_A] + \frac{\omega_B^3 e^{-(\Gamma_A+\Gamma_b)T/2}}{c^4\epsilon_0^2\hbar}\left[2\cos(\Delta_{AB}T) - \frac{\Gamma_A+\Gamma_b}{\Delta_{AB}}\sin(\Delta_{AB}T)\right] \\ & \times [\boldsymbol{\mu}_A \wedge \boldsymbol{\nabla} \wedge \mathrm{Re}\,\mathbb{G}(k_B R)\cdot\boldsymbol{\mu}_b\boldsymbol{\mu}_b\cdot \mathrm{Re}\,\mathbb{G}(k_B R)\cdot\boldsymbol{\mu}_A - \boldsymbol{\mu}_A \wedge \boldsymbol{\nabla} \wedge \mathrm{Im}\,\mathbb{G}(k_B R)\cdot\boldsymbol{\mu}_b\boldsymbol{\mu}_b\cdot \mathrm{Im}\,\mathbb{G}(k_B R)\cdot\boldsymbol{\mu}_A]\Bigg\}, \end{aligned} \tag{7}$$

$$\begin{aligned}\langle \mathbf{F}_B^{nc}\rangle \simeq \sum_b \Bigg\{ & \frac{2\omega_A^3\Gamma_A e^{-\Gamma_A T}}{c^4\epsilon_0^2\hbar\Delta_{AB}}[\boldsymbol{\mu}_b \wedge \boldsymbol{\nabla} \wedge \mathrm{Re}\,\mathbb{G}(k_A R)\cdot\boldsymbol{\mu}_A\boldsymbol{\mu}_b\cdot \mathrm{Im}\,\mathbb{G}(k_A R)\cdot\boldsymbol{\mu}_A - \boldsymbol{\mu}_b \wedge \boldsymbol{\nabla} \wedge \mathrm{Im}\,\mathbb{G}(k_A R)\cdot\boldsymbol{\mu}_A\boldsymbol{\mu}_b\cdot \mathrm{Re}\,\mathbb{G}(k_A R)\cdot\boldsymbol{\mu}_A] \\ & - \frac{\omega_A\omega_B^2 e^{-(\Gamma_A+\Gamma_b)T/2}}{c^4\epsilon_0^2\hbar}\left[2\sin(\Delta_{AB}T) + \frac{\Gamma_A+\Gamma_b}{\Delta_{AB}}\cos(\Delta_{AB}T)\right] \\ & \times [\boldsymbol{\mu}_b \wedge \boldsymbol{\nabla} \wedge \mathrm{Re}\,\mathbb{G}(k_A R)\cdot\boldsymbol{\mu}_A\boldsymbol{\mu}_b\cdot \mathrm{Im}\,\mathbb{G}(k_B R)\cdot\boldsymbol{\mu}_A - \boldsymbol{\mu}_b \wedge \boldsymbol{\nabla} \wedge \mathrm{Im}\,\mathbb{G}(k_A R)\cdot\boldsymbol{\mu}_A\boldsymbol{\mu}_b\cdot \mathrm{Re}\,\mathbb{G}(k_B R)\cdot\boldsymbol{\mu}_A] \\ & + \frac{\omega_A\omega_B^2 e^{-(\Gamma_A+\Gamma_b)T/2}}{c^4\epsilon_0^2\hbar}\left[2\cos(\Delta_{AB}T) - \frac{\Gamma_A+\Gamma_b}{\Delta_{AB}}\sin(\Delta_{AB}T)\right] \\ & \times [\boldsymbol{\mu}_b \wedge \boldsymbol{\nabla} \wedge \mathrm{Re}\,\mathbb{G}(k_A R)\cdot\boldsymbol{\mu}_A\boldsymbol{\mu}_b\cdot \mathrm{Re}\,\mathbb{G}(k_B R)\cdot\boldsymbol{\mu}_A + \boldsymbol{\mu}_b \wedge \boldsymbol{\nabla} \wedge \mathrm{Im}\,\mathbb{G}(k_A R)\cdot\boldsymbol{\mu}_A\boldsymbol{\mu}_b\cdot \mathrm{Im}\,\mathbb{G}(k_B R)\cdot\boldsymbol{\mu}_A]\Bigg\}. \end{aligned} \tag{8}$$

In these equations $\mathbf{R} = \mathbf{R}_A - \mathbf{R}_B$, $\boldsymbol{\mu}_A = \langle A_-|\mathbf{d}_A|A_+\rangle$, $\boldsymbol{\mu}_b = \langle B_-|\mathbf{d}_B|b\rangle$, and $\mathbb{G}(kr)$ is the dyadic Green's function of the electric field induced at $\mathbf{r}$ by an electric dipole of frequency ck at the origin,

$$\mathbb{G}(kr) = \frac{k\, e^{ikr}}{-4\pi}[\alpha/kr + i\beta/(kr)^2 - \beta/(kr)^3], \tag{9}$$

with $\alpha = \mathbb{I} - \hat{\mathbf{r}}\hat{\mathbf{r}}$, $\beta = \mathbb{I} - 3\hat{\mathbf{r}}\hat{\mathbf{r}}$, and $\hat{\mathbf{r}}$ being a unitary vector along $\mathbf{r}$. Higher-order contributions of the rest of the diagrams in Fig. 7, which contain both fully resonant and semiresonant terms, are given in detail in Appendix A, Eqs. (A3) and (A4).

IV. NONCONSERVATIVE FORCES ON IDENTICAL ATOMS

We proceed to take the identical-atom limit upon Eqs. (7) and (8) obtained in the previous section considering $\Gamma_A \to \Gamma_b \equiv \Gamma_0$, $\omega_A \to \omega_B \equiv \omega_0$, and $\Delta_{AB}/\Gamma_0 \to 0$. In order for the computations of Sec. III to remain valid in this limit, the observation time T must be small in comparison to the time that it takes for the excitation to be transferred from atom A to atom B, i.e., $\sum_b k_0^2 \boldsymbol{\mu}_A \cdot \mathrm{Re}\,\mathbb{G}(k_0R)\cdot\boldsymbol{\mu}_b \leqslant \hbar\epsilon_0/T$ [16,28]. This is the weak-interaction regime, which implies that the original atomic states are quasistationary despite the degeneracy of the system. In addition, as mentioned in the Introduction, the distinct feature of the nonconservative forces is the presence of components which are orthogonal to the interatomic axis. These components are indeed proportional to the components of the transition dipole moments which are perpendicular to the axial vector $\mathbf{R}$. We will denote them with a superscript $\perp$, whereas those along $\mathbf{R}$ will be denoted with a superscript $\parallel$. That is, $\mu^{\parallel}_{A,b} = \boldsymbol{\mu}_{A,b}\cdot\hat{\mathbf{R}}$, $\boldsymbol{\mu}^{\perp}_{A,b} = \alpha\cdot\boldsymbol{\mu}_{A,b}$, where α is the projector tensor defined below Eq. (9).

All in all, taking the identical-atom limit on Eqs. (7) and (8), the dominant contributions to the nonconservative forces on each atom read

$$\begin{aligned}\langle \mathbf{F}^{nc}_A\rangle &= \frac{2\omega_0^4(1-\Gamma_0 T)e^{-\Gamma_0 T}}{-c^5\epsilon_0^2\hbar}\sum_b[\mu^{\parallel}_A\boldsymbol{\mu}^{\perp}_b - \mu^{\perp}_A\mu^{\perp}_b\hat{\mathbf{R}}]\\ &\quad\times\boldsymbol{\mu}_A\cdot[\mathrm{Re}\,\mathcal{G}(k_0R)\mathrm{Im}\,\mathbb{G}(k_0R)\\ &\quad+\mathrm{Im}\,\mathcal{G}(k_0R)\mathrm{Re}\,\mathbb{G}(k_0R)]\cdot\boldsymbol{\mu}_b,\\ \langle \mathbf{F}^{nc}_B\rangle &= \frac{2\omega_0^4(1-\Gamma_0 T)e^{-\Gamma_0 T}}{c^5\epsilon_0^2\hbar}\sum_b[\mu^{\parallel}_b\boldsymbol{\mu}^{\perp}_A - \mu^{\perp}_A\mu^{\perp}_b\hat{\mathbf{R}}]\\ &\quad\times\boldsymbol{\mu}_A\cdot[\mathrm{Re}\,\mathcal{G}(k_0R)\mathrm{Im}\,\mathbb{G}(k_0R)\\ &\quad-\mathrm{Im}\,\mathcal{G}(k_0R)\mathrm{Re}\,\mathbb{G}(k_0R)]\cdot\boldsymbol{\mu}_b,\end{aligned}\tag{10}$$

where $\mathcal{G}(kr)\mathcal{E}\cdot\hat{\mathbf{r}}$ is the dyadic Green's tensor of the magnetic field induced at $\mathbf{r}$ by an electric dipole of frequency ck at the origin [3] with $\boldsymbol{\nabla}\times\mathbb{G}(kR) = ik\mathcal{G}(kR)\mathcal{E}\cdot\hat{\mathbf{R}}$, $\mathcal{E}$ being the three-dimensional Levi-Civita tensor, and

$$\mathcal{G}(kr) = -\frac{ke^{ikr}}{4\pi}\left(\frac{1}{kr}+\frac{i}{(kr)^2}\right).\tag{11}$$

Higher-order terms in $\langle\mathbf{F}^{nc}_{A,B}\rangle$ are Γ_0/ω_0 and R/cT times smaller—see Appendix B, Eqs. (B1) and (B2).

Next, substituting Eqs. (9) and (11) into Eq. (10) one obtains that as with the conservative vdW forces, $\langle\mathbf{F}^{nc}_A\rangle$ oscillates in space with wavelength π/k_0,

$$\begin{aligned}\langle \mathbf{F}^{nc}_A\rangle &= \frac{k_0^6(1-\Gamma_0 T)e^{-\Gamma_0 T}}{-8\pi^2\epsilon_0^2\hbar c}\sum_b[\mu^{\parallel}_A\boldsymbol{\mu}^{\perp}_b - \mu^{\perp}_A\mu^{\perp}_b\hat{\mathbf{R}}]\\ &\quad\times\boldsymbol{\mu}_A\cdot\left[\frac{\alpha}{(k_0R)^2}\left(\sin(2k_0R)+\frac{\cos(2k_0R)}{k_0R}\right)+\frac{\beta}{(k_0R)^3}\right.\\ &\quad\left.\times\left(\cos(2k_0R)-\frac{2\,\sin(2k_0R)}{k_0R}-\frac{\cos(2k_0R)}{(k_0R)^2}\right)\right]\cdot\boldsymbol{\mu}_b,\end{aligned}\tag{12}$$

whereas $\langle\mathbf{F}^{nc}_B\rangle$ decreases monotonically with R,

$$\begin{aligned}\langle \mathbf{F}^{nc}_B\rangle &= \frac{k_0^6(1-\Gamma_0 T)e^{-\Gamma_0 T}}{8\pi^2\epsilon_0^2\hbar c}\sum_b\left[\mu^{\parallel}_b\boldsymbol{\mu}^{\perp}_A - \mu^{\perp}_A\mu^{\perp}_b\hat{\mathbf{R}}\right]\\ &\quad\times\boldsymbol{\mu}_A\cdot\left[\frac{\beta-\alpha}{(k_0R)^3}+\frac{\beta}{(k_0R)^5}\right]\cdot\boldsymbol{\mu}_b.\end{aligned}\tag{13}$$

As advanced, in contrast to the conservative vdW forces, the most remarkable feature of the nonconservative forces is the presence of components which are perpendicular to the interatomic axis. Also, as with the vdW forces, nonconservative forces possess reciprocal and nonreciprocal components [26–28]. The former, $\pm\langle\mathbf{F}^{nc}_A - \mathbf{F}^{nc}_B\rangle/2$, satisfy the ordinary action reaction principle; whereas the latter amount to a net force on the two-atom system, $\langle\mathbf{F}^{nc}_A + \mathbf{F}^{nc}_B\rangle$,

$$\begin{aligned}\langle \mathbf{F}^{nc}_A + \mathbf{F}^{nc}_B\rangle &= \frac{2\omega_0^4(1-\Gamma_0 T)e^{-\Gamma_0 T}}{-c^5\epsilon_0^2\hbar}\sum_b[\mu^{\parallel}_A\boldsymbol{\mu}^{\perp}_b + \mu^{\parallel}_b\boldsymbol{\mu}^{\perp}_A\\ &\quad-2\mu^{\perp}_A\mu^{\perp}_b\hat{\mathbf{R}}]\boldsymbol{\mu}_A\cdot\mathrm{Im}\,\mathcal{G}(k_0R)\mathrm{Re}\,\mathbb{G}(k_0R)\cdot\boldsymbol{\mu}_b\\ &\quad+[\mu^{\parallel}_A\boldsymbol{\mu}^{\perp}_b - \mu^{\parallel}_b\boldsymbol{\mu}^{\perp}_A]\boldsymbol{\mu}_A\cdot\mathrm{Re}\,\mathcal{G}(k_0R)\mathrm{Im}\,\mathbb{G}(k_0R)\\ &\quad\cdot\boldsymbol{\mu}_b,\end{aligned}\tag{14}$$

which oscillates in space as $\sim\sin(2k_0R)/(k_0R)^2$ in the retarded regime.

The strength of the nonconservative forces in the perturbative regime is of an order Γ_0/ω_0 weaker than that of the vdW forces [28]. Hence, the components along the interatomic axis are hardly distinguishable experimentally. On the contrary, their orthogonal components, absent in the vdW forces, might be observed. The orthogonal components of the reciprocal forces generate a torque around the center of mass, whereas the net force of Eq. (14) displaces the center of mass as illustrated in Fig. 1.

Nonconservative forces on Dicke states

For the sake of completeness, let us compute the nonconservative forces upon the atoms in Dicke states. Under the perturbative condition $k_0R \gtrsim 1$, it is possible to excite the system suddenly and delocalizing the excitation symmetrically between both atoms. Thus, the symmetric $(+)$ and antisymmetric $(-)$ Dicke states read

$$|\Psi_\pm(0)\rangle = [|A_+\rangle\otimes|B_-\rangle \pm |A_-\rangle\otimes|B_+\rangle]\otimes|0_\gamma\rangle/\sqrt{2}.\tag{15}$$

The collective interaction of atomic systems in Dicke states with the environment has been studied in a number of articles—-cf. Refs. [37,38]. In the present case, we concentrate on the internal forces. The most important difference with respect to our previous calculation on nonsymmetrically excited atoms is the absence of nonreciprocal forces. This is a direct consquence of the parity symmetry of the Dicke states. As for the existence of nonconservative forces, despite being stationary states, resonant photons fly continuously between the two atoms of Dicke states. This not only induces an additional variation on the phase of the two-atom wave function, but also a time variation on the longitudinal momentum associated with the transfer of the resonant photons. The computation of the forces in either Dicke state involves now

two kinds of diagrams. The first kind is made of diagrams of order W^4, which are common to the symmetric and antisymmetric states, and are equivalent to the diagrams of Fig. 7 for nonsymmetrically excited atoms. Using the nomenclature of the precedent section and denoting the order of the interaction with a superscript within parentheses, the contribution of diagrams of order W^4 to the forces on each atom in either Dicke state is

$$\begin{aligned}\langle \mathbf{F}^{(4)\pm}_{A,B}\rangle &= \pm\big(\langle \mathbf{F}^{nc}_{A}\rangle - \langle \mathbf{F}^{nc}_{B}\rangle\big)/2\\ &= \mp\frac{\omega_0^4(1-\Gamma_0 T)e^{-\Gamma_0 T}}{c^5\epsilon_0^2\hbar}\sum_b \big[\mu_A^{\parallel}\boldsymbol{\mu}_b^{\perp}+\mu_b^{\parallel}\boldsymbol{\mu}_A^{\perp}-2\mu_A^{\perp}\mu_b^{\perp}\hat{\mathbf{R}}\big]\boldsymbol{\mu}_A\cdot \mathrm{Re}\,\mathcal{G}(k_0R)\mathrm{Im}\,\mathbb{G}(k_0R)\cdot\boldsymbol{\mu}_b\\ &\quad+\big[\mu_A^{\parallel}\boldsymbol{\mu}_b^{\perp}-\mu_b^{\parallel}\boldsymbol{\mu}_A^{\perp}\big]\boldsymbol{\mu}_A\cdot \mathrm{Im}\,\mathcal{G}(k_0R)\mathrm{Re}\,\mathbb{G}(k_0R)\cdot\boldsymbol{\mu}_b,\end{aligned}\tag{16}$$

where the + sign on the right-hand side of the first equality applies to the force on atom A whereas the − sign applies to B, respectively.

As for the contribution of the diagrams of the second kind, of order W^2, they are depicted in Fig. 4, and their contribution to the nonconservative forces presents opposite signs for symmetric and antisymmetric states,

$$\langle \mathbf{F}^{(2)\pm}_{A,B}\rangle = (\pm)\times(\pm)\frac{\omega_0^2\Gamma_0 e^{-\Gamma_0 T}}{c^3\epsilon_0}\big[\mu_A^{\parallel}\boldsymbol{\mu}_A^{\perp}-(\mu_A^{\perp})^2\hat{\mathbf{R}}\big]\mathrm{Re}\,\mathcal{G}(k_0R).\tag{17}$$

In this equation the first ± signs on the right-hand side of the equality correspond to symmetric and antisymmetric states, whereas the second ± signs refer to atoms A and B, respectively. The same as for the forces of order W^4, the forces of order W^2 are also reciprocal. Putting all the contributions together, we end up with the expressions,

$$\begin{aligned}\langle \mathbf{F}^{\pm}_{A}\rangle &= -\langle \mathbf{F}^{\pm}_{B}\rangle\\ &= \mp\frac{k_0^6(1-\Gamma_0 T)e^{-\Gamma_0 T}}{8\pi^2\epsilon_0^2\hbar c}\sum_b\Bigg\{\mu_A^{\parallel}\boldsymbol{\mu}_b^{\perp}\boldsymbol{\mu}_A\cdot\Bigg[\frac{\alpha}{(k_0R)^2}\bigg(\sin(2k_0R)+\frac{\cos(2k_0R)}{k_0R}\bigg)\\ &\quad+\frac{\beta}{(k_0R)^3}\bigg(\cos(2k_0R)-\frac{2\sin(2k_0R)}{k_0R}-\frac{\cos(2k_0R)}{(k_0R)^2}\bigg)\Bigg]\cdot\boldsymbol{\mu}_b+\mu_b^{\parallel}\boldsymbol{\mu}_A^{\perp}\boldsymbol{\mu}_A\cdot\Bigg[\frac{\beta-\alpha}{(k_0R)^3}+\frac{\beta}{(k_0R)^5}\Bigg]\cdot\boldsymbol{\mu}_b-\mu_A^{\perp}\mu_b^{\perp}\hat{\mathbf{R}}\boldsymbol{\mu}_A\\ &\quad\cdot\Bigg[\frac{\alpha}{(k_0R)^2}\bigg(\sin(2k_0R)+\frac{\cos(2k_0R)-1}{k_0R}\bigg)+\frac{\beta}{(k_0R)^3}\bigg(1+\cos(2k_0R)-\frac{2\sin(2k_0R)}{k_0R}-\frac{\cos(2k_0R)-1}{(k_0R)^2}\bigg)\Bigg]\cdot\boldsymbol{\mu}_b\Bigg\}\\ &\quad\mp\frac{k_0^3\Gamma_0 e^{-\Gamma_0 T}}{\epsilon_0 c}[\mu_A^{\parallel}\boldsymbol{\mu}_A^{\perp}-(\mu_A^{\perp})^2\hat{\mathbf{R}}]\bigg[\frac{\cos(k_0R)}{k_0R}-\frac{\sin(k_0R)}{(k_0R)^2}\bigg].\end{aligned}\tag{18}$$

For the sake of comparison, we represent in Fig. 5 the strength of the nonconservative forces of order W^4 and order W^2 in terms of the interatomic distance. We observe that whereas the forces of order W^2 are dominant in the far field, those of order W^4 tend to diverge at short distances.

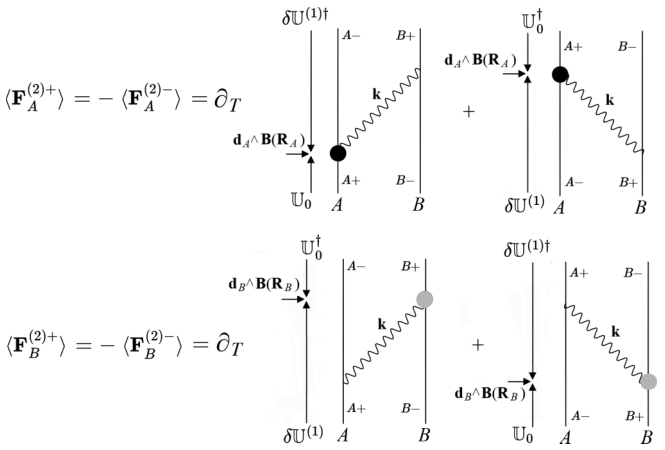

FIG. 4. Diagrammatic representation of the two processes which contribute to $\langle \mathbf{F}^{(2)\pm}_{A,B}\rangle$. The big circles in black and gray stand for the insertion of the Schrödinger operators $\mathbf{d}_{A,B}\wedge\mathbf{B}(\mathbf{R}_{A,B})$, respectively, whose expectation values are computed.

V. TRANSVERSE DISPLACEMENT OF A BINARY SYSTEM OF HYDROGEN ATOMS

We finalize with the estimate of the displacement caused on an excited binary system of hydrogen atoms by the orthogonal components of the nonconservative forces. Without loss of generality, let us consider that initially one of the atoms, say atom A, is excited to the energy-level $n=2$, $l=1$ in state $|A_+\rangle = |2p_z - i2p_y\rangle/\sqrt{2}$, whereas atom B is in the ground-state $|1S\rangle$. The atoms are placed a distance R apart along the $\hat{\mathbf{z}}$ axis with R being large enough to be considered as constant all along the observation time, in the weak interaction regime—see Fig. 1. We are interested in the transverse displacement of each atom, $\mathbf{S}^{\perp}_{A,B}$, say along the $\hat{\mathbf{x}}$ axis, in a time interval slightly longer than a lifetime, $\Gamma_0^{-1}\simeq 1.6$ ns. In the first place, it is straightforward to integrate the time-dependent factors of the accelerations induced by the nonconservative forces of

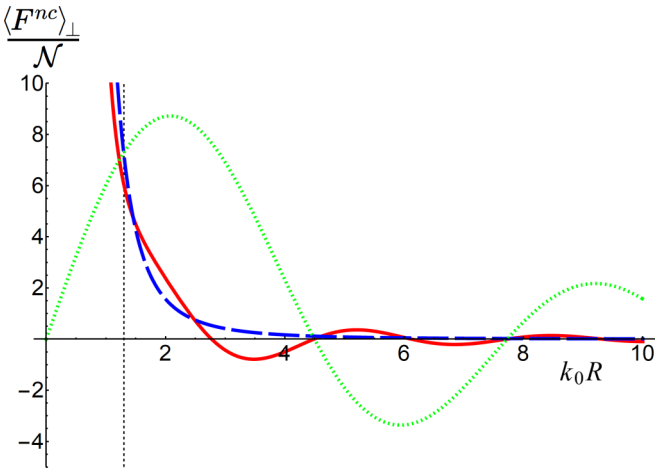

FIG. 5. Graphical representation of the spatial behavior of the components of nonconservative forces for identical atoms in Dicke states. The solid line in red represents $\mathrm{Tr}\{\langle \mathbf{F}_A^{nc}\rangle \cdot \alpha\}$, whereas the dashed line in blue is for $\mathrm{Tr}\{\langle \mathbf{F}_B^{nc}\rangle \cdot \alpha\}$, and the dotted line in green is for $\mathrm{Tr}\{\langle \mathbf{F}_A^{(2)+}\rangle \cdot \alpha\}$. The curves are normalized to $\mathcal{N} = \frac{k_0^6|\boldsymbol{\mu}|^4}{80\pi^2\epsilon_0^2\hbar c}$ for $\Gamma_0 T \ll 1$, and transition dipole moments are considered isotropic. The vertical dotted line signals the limit of the perturbative regime $k_0R \sim 1$.

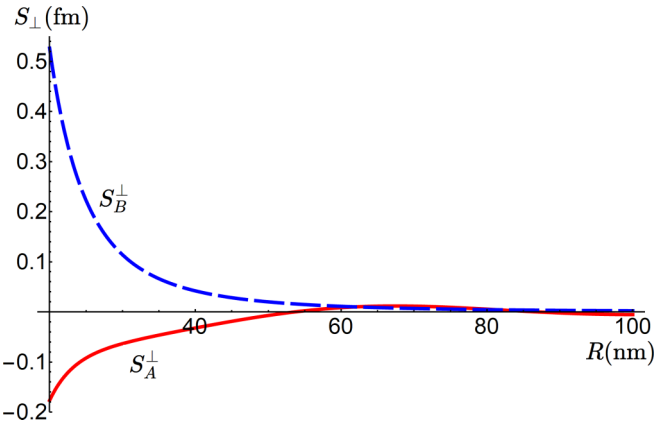

FIG. 6. Graphical representation of the perpendicular displacements along the x axis caused by the nonconservative dipole forces on a binary system of Hydrogen atoms, with one of them, A, initially excited to state $|2p_z - i2p_y\rangle/\sqrt{2}$, as a function of the interatomic distance R along the z axis. The solid line in red represents $S_A^\perp$, whereas the dashed line in blue is for $S_B^\perp$, according to Eq. (22).

Eqs. (10)–(13) in a time-interval $T \gtrsim \Gamma_0^{-1}$, $\int_0^T dt \int_0^t dt'(1 - \Gamma_0 t')e^{-\Gamma_0 t'} \approx \Gamma_0^{-2}$. This leads to

$$\mathbf{S}_A^\perp = \frac{-2\omega_0^4}{c^5\epsilon_0^2 m_H \hbar \Gamma_0^2} \sum_b \mu_A^\parallel \boldsymbol{\mu}_b^\perp \boldsymbol{\mu}_A \cdot [\mathrm{Re}\,\mathcal{G}(k_0R)\mathrm{Im}\,\mathbb{G}(k_0R) + \mathrm{Im}\,\mathcal{G}(k_0R)\mathrm{Re}\,\mathbb{G}(k_0R)] \cdot \boldsymbol{\mu}_b, \tag{19}$$

$$\mathbf{S}_B^\perp = \frac{2\omega_0^4}{c^5\epsilon_0^2 m_H \hbar \Gamma_0^2} \sum_b \mu_b^\parallel \boldsymbol{\mu}_A^\perp \boldsymbol{\mu}_A \cdot [\mathrm{Re}\,\mathcal{G}(k_0R)\mathrm{Im}\,\mathbb{G}(k_0R) - \mathrm{Im}\,\mathcal{G}(k_0R)\mathrm{Re}\,\mathbb{G}(k_0R)] \cdot \boldsymbol{\mu}_b, \tag{20}$$

where m_H is the mass of a hydrogen atom. Next, taking into account the transition electric dipole moments,

$$\begin{aligned} \boldsymbol{\mu}_A &= \langle 1S|\mathbf{d}_A|2p_z - i2p_y\rangle/\sqrt{2} \\ &= \frac{e\,a_0 2^7}{3^5}(\hat{\mathbf{z}} - \hat{\mathbf{x}}), \\ \sum_b \boldsymbol{\mu}_b &= \langle 1S|\mathbf{d}_B|2p_x + 2p_y + 2p_z\rangle \\ &= \frac{e\,a_0 2^{15/2}}{3^5}(\hat{\mathbf{z}} - \hat{\mathbf{x}} - \hat{\mathbf{y}}), \end{aligned} \tag{21}$$

where a_0 is Bohr's radius and e is the electronic charge, and replacing their numerical values in Eqs. (19) and (20), we end up with

$$\begin{aligned} \mathbf{S}_A^\perp &\simeq 0.15\ \mathrm{fm}\frac{(2v^2-1)\cos 2v - (2v - v^3)\sin 2v}{v^5}\hat{\mathbf{x}}, \\ \mathbf{S}_B^\perp &\simeq 0.3\ \mathrm{fm}\frac{1+v^2}{v^5}\hat{\mathbf{x}}, \quad v \equiv 2\pi R/\lambda_0 \end{aligned} \tag{22}$$

for $\lambda_0 \simeq 121.6$ nm. In order for our computation to remain perturbative, $v \gtrsim 1$, meaning that the maximum values of the perpendicular displacements are on the order of 1 fm in the weak-interaction regime—see Fig. 6. Note also that for $R \lesssim 50$ nm both atoms move in the same direction, meaning that the nonreciprocal components of the forces dominate there.

VI. CONCLUSIONS AND OUTLOOK

We have computed the nonconservative dipole forces between the two-level atoms of a suddenly excited binary system. We have particularized to the identical-atom limit, and we have considered the case of an only atom excited and the case of the atoms in Dicke states. We have found that the nonconservative forces are of an order Γ_0/ω_0 weaker than the conservative vdW forces. Nonetheless, they possess components orthogonal to the interatomic axis that might be experimentally accessible. Our perturbative computation on a binary system of hydrogen atoms with one of them initially excited, in the weak-interaction regime, shows that the orthogonal displacement of the atoms is on the order of a Fermi for interatomic distances in the middle-far field. Nevertheless, the displacements are expected to be much greater for shorter interatomic distances. In this respect, in order to facilitate its observation, Rydberg atoms present themselves as good candidates due to their strong resonant interactions at a short distance [39–45]. To this end, it will be necessary to extend the present calculations to the nonperturbative regime to account for the multiple transfer of the excitation between the atoms.

As with the vdW forces, the leading terms of the nonconservative forces are fully resonant. Whereas for atoms symmetrically excited (e.g., those in Dicke states) forces are reciprocal, when only one of the atoms is initially excited nonreciprocal forces show up which generate a net displacement of the two-atom system. On physical grounds, this can be interpreted as a result of the breaking of parity symmetry. In contrast to the net vdW force, the net nonconservative force is not related to the directionality of spontaneous emission. This is so because the net nonconservative force is not compensated by the time variation of the momentum carried by the

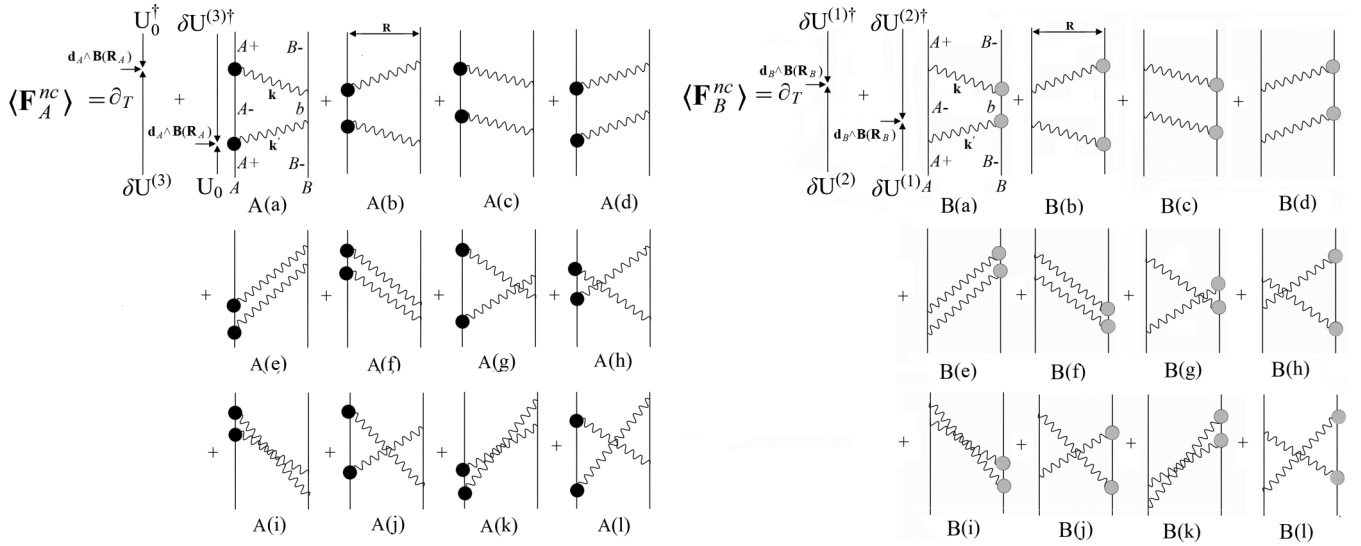

FIG. 7. Diagrammatic representation of the 12 processes which contribute to $\langle \mathbf{F}_A^{nc} \rangle$ and $\langle \mathbf{F}_B^{nc} \rangle$. The big circles in black and gray stand for the insertion of the Schrödinger operators $\mathbf{d}_{A,B} \wedge \mathbf{B}(\mathbf{R}_{A,B})$ whose expectation values are computed.

transverse photons which mediate the interaction [27], but by the time variation of the longitudinal EM momentum which is a function of the longitudinal electric field.

ACKNOWLEDGMENTS

Financial support is acknowledged from Grants No. MTM2014-57129-C2-1-P (MINECO), No. VA137G18, and No. BU229P18 (JCyL) as well as from the Spanish Ministerio de Ciencia e Innovación (MICIN) and the Consejería de Educación, Junta de Castilla y León, through the Project QCAYLE (NextGenerationEU funds, PRTRC17.I1). M.D. acknowledges the hospitality of Institut Néel, CNRS. J.S.-C. acknowledges financial support from the Doctorate Program Funds No. UVa2021 and Banco Santander.

APPENDIX A: COMPLETE EXPRESSION OF THE NONCONSERVIATIVE FORCES BETWEEN DISSIMILAR ATOMS

In this Appendix we write the complete expressions for $\langle \mathbf{F}_{A,B}^{nc} \rangle$ for dissimilar atoms. The diagrammatic representation of the processes contributing to these forces is given in Fig. 7.

In the first place, we illustrate the calculation with the detailed reading of the contribution of diagram A(a) to $\langle \mathbf{F}_A^{nc} \rangle$. It is

$$\frac{1}{\hbar^3}\frac{\partial}{\partial T}\int_0^\infty \frac{\mathcal{V}k^2\,dk}{(2\pi)^3}\int_0^\infty \frac{\mathcal{V}k'^2\,dk'}{(2\pi)^3}\int_0^{4\pi} d\Theta \int_0^{4\pi} d\Theta' \Bigg\{ \Bigg[i\langle A_+, B_-, 0_\gamma | e^{i\Omega_a^* T} | A_+, B_-, 0_\gamma \rangle \int_0^T dt \int_0^t dt' \int_0^{t'} dt''$$
$$\times \sum_b \langle A_+, B_-, 0_\gamma | \mathbf{d}_A \wedge \mathbf{B}_{\mathbf{k}}^{(-)}(\mathbf{R}_A) | A_-, B_-, \gamma_{\mathbf{k}} \rangle e^{-i\omega(T-t)} \langle A_-, B_-, \gamma_{\mathbf{k}} | \mathbf{d}_B \cdot \mathbf{E}_{\mathbf{k}}^{(+)}(\mathbf{R}_B) | A_-, b, 0_\gamma \rangle e^{-i\Omega_b(t-t')} \langle A_-, b, 0_\gamma | \mathbf{d}_B$$
$$\cdot \mathbf{E}_{\mathbf{k}'}^{(-)}(\mathbf{R}_B) | A_-, B_-, \gamma_{\mathbf{k}'} \rangle e^{-i\omega'(t'-t'')} \langle A_-, B_-, \gamma_{\mathbf{k}'} | \mathbf{d}_A \cdot \mathbf{E}_{\mathbf{k}'}^{(+)}(\mathbf{R}_A) | A_+, B_-, 0_\gamma \rangle e^{-i\Omega_a t''} \Bigg] + [k \leftrightarrow k']^\dagger \Bigg\}, \tag{A1}$$

where $|A_+, B_-, 0_\gamma\rangle$ is the initial two-atom-EM-vacuum state, $|\gamma_{\mathbf{k}}\rangle$ is a one-photon state of momentum $\mathbf{k}$ and frequency $\omega = ck$, $\mathcal{V}$ is the volume of quantization to be taken eventually to infinity, Θ and Θ' are the solid angle variables and the complex time exponentials are the result of the application of the free time-evolution operator $\mathbb{U}_0(t)$ between the interaction vertices with $\Omega_a = \omega_A - i\Gamma_A/2$ and $\Omega_b = \omega_B - i\Gamma_b/2$ where the dissipative imaginary terms account for radiative emission in the Weisskopf-Wigner approximation.

Integrating in time and solid angles the expression of Eq. (A1), one obtains

$$\frac{-c}{\hbar\pi^2\epsilon_0^2}\frac{\partial}{\partial T}\sum_b \mathrm{Re}\int_0^\infty ik\,dk\,\boldsymbol{\mu}_A \wedge \boldsymbol{\nabla} \wedge \mathrm{Im}\,\mathbb{G}(kR)\cdot\boldsymbol{\mu}_b \int_0^\infty dk' k'^2 \boldsymbol{\mu}_B \cdot \mathrm{Im}\,\mathbb{G}(k'R)\cdot\boldsymbol{\mu}_A\, e^{i\Omega_a^* T}\Bigg[\frac{e^{-i\Omega_a T}-e^{-i\omega T}}{(\omega'-\Omega_a)(\Omega_b-\Omega_a)(\omega-\Omega_a)}$$
$$-\frac{e^{-i\Omega_b T}-e^{-i\omega T}}{(\omega'-\Omega_a)(\Omega_b-\Omega_a)(\omega-\Omega_b)}+\frac{e^{-i\omega' T}-e^{-i\omega T}}{(\omega'-\Omega_a)(\omega'-\Omega_b)(\omega-\omega')}-\frac{e^{-i\Omega_b T}-e^{-i\omega T}}{(\omega'-\Omega_a)(\omega'-\Omega_b)(\omega-\Omega_b)}\Bigg], \tag{A2}$$

where $\mathbf{R} = \mathbf{R}_A - \mathbf{R}_B$, $\boldsymbol{\mu}_A = \langle A_-|\mathbf{d}_A|A_+\rangle$, $\boldsymbol{\mu}_b = \langle B_-|\mathbf{d}_B|b\rangle$, and we have used the identities,

$$\int d\Theta_{\mathbf{k}} \langle 0_\gamma|\mathbf{E}^{(-)}_{\mathbf{k}}(\mathbf{r})\,\mathbf{E}^{(+)}_{\mathbf{k}}(\mathbf{0})|0_\gamma\rangle = -\frac{8\pi^2\hbar c}{\epsilon_0}\ \mathrm{Im}\,\mathbb{G}(kr),$$
$$\int d\Theta_{\mathbf{k}} \langle 0_\gamma|\mathbf{B}^{(-)}_{\mathbf{k}}(\mathbf{r})\mathbf{E}^{(+)}_{\mathbf{k}}(\mathbf{0})|0_\gamma\rangle = -\frac{8\pi^2 i\hbar}{\epsilon_0 k}\boldsymbol{\nabla}\wedge \mathrm{Im}\,\mathbb{G}(kr).$$

Operating in a similar manner with the rest of the diagrams, upon integration in the momenta of the virtual photons k and k' on the complex plane, we arrive at

$$\begin{aligned}
\langle \mathbf{F}^{nc}_A\rangle = \sum_b \Bigg\{ & \frac{2\omega_A^3\Gamma_A e^{-\Gamma_A T}}{c^4\epsilon_0^2\hbar\Delta_{AB}}[\boldsymbol{\mu}_A\wedge\boldsymbol{\nabla}\wedge \mathrm{Re}\mathbb{G}(k_AR)\cdot\boldsymbol{\mu}_b\boldsymbol{\mu}_b\cdot \mathrm{Im}\,\mathbb{G}(k_AR)\cdot\boldsymbol{\mu}_A + \boldsymbol{\mu}_A\wedge\boldsymbol{\nabla}\wedge \mathrm{Im}\,\mathbb{G}(k_AR)\cdot\boldsymbol{\mu}_b\boldsymbol{\mu}_b\cdot \mathrm{Re}\mathbb{G}(k_AR)\cdot\boldsymbol{\mu}_A] \\
& - \frac{\omega_B^3 e^{-(\Gamma_A+\Gamma_b)T/2}}{c^4\epsilon_0^2\hbar}\left[2\sin(\Delta_{AB}T) + \frac{\Gamma_A+\Gamma_b}{\Delta_{AB}}\cos(\Delta_{AB}T)\right][\boldsymbol{\mu}_A\wedge\boldsymbol{\nabla}\wedge \mathrm{Re}\,\mathbb{G}(k_BR)\cdot\boldsymbol{\mu}_b\boldsymbol{\mu}_b\cdot \mathrm{Im}\,\mathbb{G}(k_BR)\cdot\boldsymbol{\mu}_A \\
& + \boldsymbol{\mu}_A\wedge\boldsymbol{\nabla}\wedge \mathrm{Im}\,\mathbb{G}(k_BR)\cdot\boldsymbol{\mu}_b\boldsymbol{\mu}_b\cdot \mathrm{Re}\,\mathbb{G}(k_BR)\cdot\boldsymbol{\mu}_A] + \frac{\omega_B^3 e^{-(\Gamma_A+\Gamma_b)T/2}}{c^4\epsilon_0^2\hbar}\left[2\cos(\Delta_{AB}T) - \frac{\Gamma_A+\Gamma_b}{\Delta_{AB}}\sin(\Delta_{AB}T)\right] \\
& \times[\boldsymbol{\mu}_A\wedge\boldsymbol{\nabla}\wedge \mathrm{Re}\,\mathbb{G}(k_BR)\cdot\boldsymbol{\mu}_b\boldsymbol{\mu}_b\cdot \mathrm{Re}\,\mathbb{G}(k_BR)\cdot\boldsymbol{\mu}_A - \boldsymbol{\mu}_A\wedge\boldsymbol{\nabla}\wedge \mathrm{Im}\,\mathbb{G}(k_BR)\cdot\boldsymbol{\mu}_b\boldsymbol{\mu}_b\cdot \mathrm{Im}\,\mathbb{G}(k_BR)\cdot\boldsymbol{\mu}_A] \\
& + \frac{\omega_B(\Gamma_A+\Gamma_b)e^{-(\Gamma_A+\Gamma_b)T/2}}{c^3\epsilon_0^2\hbar}[\boldsymbol{\mu}_A\wedge\boldsymbol{\nabla}\wedge \mathrm{Im}\,\mathbb{G}(k_BR)\cdot\boldsymbol{\mu}_b\cos(\Delta_{AB}T) + \boldsymbol{\mu}_A\wedge\boldsymbol{\nabla}\wedge \mathrm{Re}\,\mathbb{G}(k_BR)\cdot\boldsymbol{\mu}_b\sin(\Delta_{AB}T)] \\
& \times\int_0^\infty \frac{dq}{\pi}\frac{(q^2-k_Ak_B)q^2\boldsymbol{\mu}_A\cdot\mathbb{G}(iqR)\cdot\boldsymbol{\mu}_b}{(q^2+k_A^2)(q^2+k_B^2)} + \frac{2\omega_B\Delta_{AB}e^{-(\Gamma_A+\Gamma_b)T/2}}{c^3\epsilon_0^2\hbar}[\boldsymbol{\mu}_A\wedge\boldsymbol{\nabla}\wedge \mathrm{Im}\,\mathbb{G}(k_BR)\cdot\boldsymbol{\mu}_b\sin(\Delta_{AB}T) \\
& - \boldsymbol{\mu}_A\wedge\boldsymbol{\nabla}\wedge \mathrm{Re}\,\mathbb{G}(k_BR)\cdot\boldsymbol{\mu}_b\cos(\Delta_{AB}T)]\int_0^\infty \frac{dq}{\pi}\frac{(q^2-k_Ak_B)q^2\boldsymbol{\mu}_A\cdot\mathbb{G}(iqR)\cdot\boldsymbol{\mu}_b}{(q^2+k_A^2)(q^2+k_B^2)}\Bigg\},
\end{aligned} \tag{A3}$$

$$\begin{aligned}
\langle \mathbf{F}^{nc}_B\rangle = \sum_b \Bigg\{ & \frac{2\omega_A^3\Gamma_A e^{-\Gamma_A T}}{c^4\epsilon_0^2\hbar\Delta_{AB}}[\boldsymbol{\mu}_b\wedge\boldsymbol{\nabla}\wedge \mathrm{Re}\,\mathbb{G}(k_AR)\cdot\boldsymbol{\mu}_A\boldsymbol{\mu}_b\cdot \mathrm{Im}\,\mathbb{G}(k_AR)\cdot\boldsymbol{\mu}_A - \boldsymbol{\mu}_b\wedge\boldsymbol{\nabla}\wedge \mathrm{Im}\,\mathbb{G}(k_AR)\cdot\boldsymbol{\mu}_A\boldsymbol{\mu}_b\cdot \mathrm{Re}\,\mathbb{G}(k_AR)\cdot\boldsymbol{\mu}_A] \\
& - \frac{\omega_A\omega_B^2 e^{-(\Gamma_A+\Gamma_b)T/2}}{c^4\epsilon_0^2\hbar}\left[2\sin(\Delta_{AB}T) + \frac{\Gamma_A+\Gamma_b}{\Delta_{AB}}\cos(\Delta_{AB}T)\right][\boldsymbol{\mu}_b\wedge\boldsymbol{\nabla}\wedge \mathrm{Re}\mathbb{G}(k_AR)\cdot\boldsymbol{\mu}_A\boldsymbol{\mu}_b\cdot \mathrm{Im}\,\mathbb{G}(k_BR)\cdot\boldsymbol{\mu}_A \\
& - \boldsymbol{\mu}_b\wedge\boldsymbol{\nabla}\wedge \mathrm{Im}\,\mathbb{G}(k_AR)\cdot\boldsymbol{\mu}_A\boldsymbol{\mu}_b\cdot \mathrm{Re}\,\mathbb{G}(k_BR)\cdot\boldsymbol{\mu}_A] + \frac{\omega_A\omega_B^2 e^{-(\Gamma_A+\Gamma_b)T/2}}{c^4\epsilon_0^2\hbar}\left[2\cos(\Delta_{AB}T) - \frac{\Gamma_A+\Gamma_b}{\Delta_{AB}}\sin(\Delta_{AB}T)\right] \\
& \times[\boldsymbol{\mu}_b\wedge\boldsymbol{\nabla}\wedge \mathrm{Re}\,\mathbb{G}(k_AR)\cdot\boldsymbol{\mu}_A\boldsymbol{\mu}_b\cdot \mathrm{Re}\,\mathbb{G}(k_BR)\cdot\boldsymbol{\mu}_A + \boldsymbol{\mu}_b\wedge\boldsymbol{\nabla}\wedge \mathrm{Im}\,\mathbb{G}(k_AR)\cdot\boldsymbol{\mu}_A\boldsymbol{\mu}_b\cdot \mathrm{Im}\,\mathbb{G}(k_BR)\cdot\boldsymbol{\mu}_A] \\
& - \frac{2\omega_A^3\Gamma_A e^{-\Gamma_A T}}{c^4\epsilon_0^2\hbar(\omega_A+\omega_B)}[\boldsymbol{\mu}_b\wedge\boldsymbol{\nabla}\wedge \mathrm{Re}\,\mathbb{G}(k_AR)\cdot\boldsymbol{\mu}_A\boldsymbol{\mu}_b\cdot(k_AR)\cdot\boldsymbol{\mu}_A - \boldsymbol{\mu}_b\wedge\boldsymbol{\nabla}\wedge \mathrm{Im}\,\mathbb{G}(k_AR)\cdot\boldsymbol{\mu}_A\boldsymbol{\mu}_b\cdot \mathrm{Re}\mathbb{G}(k_AR)\cdot\boldsymbol{\mu}_A] \\
& - \frac{\omega_A(\Gamma_A+\Gamma_b)e^{-(\Gamma_A+\Gamma_b)T/2}}{c^3\epsilon_0^2\hbar}[\boldsymbol{\mu}_b\wedge\boldsymbol{\nabla}\wedge \mathrm{Im}\,\mathbb{G}(k_AR)\cdot\boldsymbol{\mu}_A\cos(\Delta_{AB}T) - \boldsymbol{\mu}_b\wedge\boldsymbol{\nabla}\wedge \mathrm{Re}\,\mathbb{G}(k_AR)\cdot\boldsymbol{\mu}_A\sin(\Delta_{AB}T)] \\
& \times\int_0^\infty \frac{dq}{\pi}\frac{(q^2-k_Ak_B)q^2\boldsymbol{\mu}_A\cdot\mathbb{G}(iqR)\cdot\boldsymbol{\mu}_b}{(q^2+k_A^2)(q^2+k_B^2)} - \frac{2\omega_A\Delta_{AB}e^{-(\Gamma_A+\Gamma_b)T/2}}{c^3\epsilon_0^2\hbar}[\boldsymbol{\mu}_b\wedge\boldsymbol{\nabla}\wedge \mathrm{Im}\,\mathbb{G}(k_AR)\cdot\boldsymbol{\mu}_A\sin(\Delta_{AB}T) \\
& + \boldsymbol{\mu}_b\wedge\boldsymbol{\nabla}\wedge \mathrm{Re}\,\mathbb{G}(k_AR)\cdot\boldsymbol{\mu}_A\cos(\Delta_{AB}T)]\int_0^\infty \frac{dq}{\pi}\frac{(q^2-k_Ak_B)q^2\boldsymbol{\mu}_A\cdot\mathbb{G}(iqR)\cdot\boldsymbol{\mu}_b}{(q^2+k_A^2)(q^2+k_B^2)}\Bigg\}.
\end{aligned} \tag{A4}$$

The time oscillating terms of frequency Δ_{AB} arise from diagrams A(a) and B(a). As mentioned in Sec. III, they contain the dominant contribution for $|\Delta_{AB}| \ll \omega_{A,B}$ together with terms of an order $\Gamma_{A,b}/\Delta_{AB}$ smaller. In addition, the quasistationary terms, of an order $\Gamma_{A,b}/\omega_{A,B}$ less, come from diagrams A(g) and B(g), and semiresonant terms arise from diagrams A(c) and B(c) and A(d) and B(d). Fast oscillating spurious terms of frequency $(\omega_A+\omega_B)$ which arise from diagrams A(k) and B(k) and A(l) and B(l) are neglected. Note that, in contrast to the conservative vdW forces, there are no fully off-resonant components.

APPENDIX B: COMPLETE EXPRESSION OF THE NONCONSERVATIVE FORCES BETWEEN IDENTICAL ATOMS

In this Appendix we write the complete expressions for $\langle \mathbf{F}^{nc}_{A,B} \rangle$ for identical atoms, i.e., taking the limit $\Gamma_A \to \Gamma_b \equiv \Gamma_0$, $\omega_A \to \omega_B \equiv \omega_0$, and $\Delta_{AB}/\Gamma_0 \to 0$ upon Eqs. (A3) and (A4),

$$\begin{aligned}\langle \mathbf{F}^{nc}_{A} \rangle = \sum_b \Bigg\{ & \frac{2\Gamma_0 e^{-\Gamma_0 T}}{c^4 \epsilon_0^2 \hbar} \frac{\partial}{\partial \omega} [\omega^3 [\boldsymbol{\mu}_A \wedge \boldsymbol{\nabla} \wedge \mathrm{Re}\, \mathbb{G}(kR) \cdot \boldsymbol{\mu}_b \boldsymbol{\mu}_b \cdot \mathrm{Im}\, \mathbb{G}(kR) \cdot \boldsymbol{\mu}_A + \boldsymbol{\mu}_A \wedge \boldsymbol{\nabla} \wedge \mathrm{Im}\, \mathbb{G}(kR) \cdot \boldsymbol{\mu}_b \\ & \times \boldsymbol{\mu}_b \cdot \mathrm{Re}\, \mathbb{G}(kR) \cdot \boldsymbol{\mu}_A]]_{\omega=\omega_0} + \frac{2\omega_0^3 (1-\Gamma_0 T) e^{-\Gamma_0 T}}{c^4 \epsilon_0^2 \hbar} [\boldsymbol{\mu}_A \wedge \boldsymbol{\nabla} \wedge \mathrm{Re}\, \mathbb{G}(k_0 R) \cdot \boldsymbol{\mu}_b \boldsymbol{\mu}_b \cdot \mathrm{Re}\, \mathbb{G}(k_0 R) \cdot \boldsymbol{\mu}_A - \boldsymbol{\mu}_A \\ & \wedge \boldsymbol{\nabla} \wedge \mathrm{Im}\, \mathbb{G}(k_0 R) \cdot \boldsymbol{\mu}_b \boldsymbol{\mu}_b \cdot \mathrm{Im}\, \mathbb{G}(k_0 R) \cdot \boldsymbol{\mu}_A] - \frac{2\omega_0^2 \Gamma_0 e^{-\Gamma_0 T}}{c^4 \epsilon_0^2 \hbar} [\boldsymbol{\mu}_A \wedge \boldsymbol{\nabla} \wedge \mathrm{Re}\, \mathbb{G}(k_0 R) \cdot \boldsymbol{\mu}_b \boldsymbol{\mu}_b \cdot \mathrm{Im}\, \mathbb{G}(k_0 R) \cdot \boldsymbol{\mu}_A + \boldsymbol{\mu}_A \wedge \boldsymbol{\nabla} \\ & \wedge \mathrm{Im}\, \mathbb{G}(k_0 R) \cdot \boldsymbol{\mu}_b \boldsymbol{\mu}_b \cdot \mathrm{Re}\, \mathbb{G}(k_0 R) \cdot \boldsymbol{\mu}_A] + \frac{2\omega_0 \Gamma_0 e^{-\Gamma_0 T}}{c^3 \epsilon_0^2 \hbar} \boldsymbol{\mu}_A \wedge \boldsymbol{\nabla} \wedge \mathrm{Im}\, \mathbb{G}(k_0 R) \cdot \boldsymbol{\mu}_b \int_0^\infty \frac{dq}{\pi} \frac{(q^2 - k_0^2) q^2 \boldsymbol{\mu}_A \cdot \mathbb{G}(iqR) \cdot \boldsymbol{\mu}_b}{\left(q^2 + k_0^2\right)^2} \Bigg\}, \end{aligned} \tag{B1}$$

$$\begin{aligned}\langle \mathbf{F}^{nc}_{B} \rangle = \sum_b \Bigg\{ & \frac{2\Gamma_0 \omega_0 e^{-\Gamma_0 T}}{c^4 \epsilon_0^2 \hbar} [\boldsymbol{\mu}_b \wedge \boldsymbol{\nabla} \wedge \mathrm{Re}\, \mathbb{G}(k_0 R) \cdot \boldsymbol{\mu}_A \frac{\partial}{\partial \omega} [\omega^2 \boldsymbol{\mu}_b \cdot \mathrm{Im}\, \mathbb{G}(kR) \cdot \boldsymbol{\mu}_A]_{\omega=\omega_0} + \boldsymbol{\mu}_b \wedge \boldsymbol{\nabla} \wedge \mathrm{Im}\, \mathbb{G}(k_0 R) \\ & \cdot \boldsymbol{\mu}_A \frac{\partial}{\partial \omega} [\omega^2 \boldsymbol{\mu}_b \cdot \mathrm{Re}\, \mathbb{G}(kR) \cdot \boldsymbol{\mu}_A]_{\omega=\omega_0}] + \frac{2\omega_0^3 (1-\Gamma_0 T) e^{-\Gamma_0 T}}{c^4 \epsilon_0^2 \hbar} [\boldsymbol{\mu}_b \wedge \boldsymbol{\nabla} \wedge \mathrm{Re}\, \mathbb{G}(k_0 R) \cdot \boldsymbol{\mu}_A \boldsymbol{\mu}_b \cdot \mathrm{Re}\, \mathbb{G}(k_0 R) \cdot \boldsymbol{\mu}_A + \boldsymbol{\mu}_b \\ & \wedge \boldsymbol{\nabla} \wedge \mathrm{Im}\, \mathbb{G}(k_0 R) \cdot \boldsymbol{\mu}_A \boldsymbol{\mu}_b \cdot \mathrm{Im}\, \mathbb{G}(k_0 R) \cdot \boldsymbol{\mu}_A] - \frac{2\omega_0^2 \Gamma_0 e^{-\Gamma_0 T}}{c^4 \epsilon_0^2 \hbar} [\boldsymbol{\mu}_b \wedge \boldsymbol{\nabla} \wedge \mathrm{Re}\, \mathbb{G}(k_0 R) \cdot \boldsymbol{\mu}_A \boldsymbol{\mu}_b \cdot \mathrm{Im}\, \mathbb{G}(k_0 R) \cdot \boldsymbol{\mu}_A - \boldsymbol{\mu}_b \wedge \boldsymbol{\nabla} \\ & \wedge \mathrm{Im}\, \mathbb{G}(k_0 R) \cdot \boldsymbol{\mu}_A \boldsymbol{\mu}_b \cdot \mathrm{Re} \mathbb{G}(k_0 R) \cdot \boldsymbol{\mu}_A] - \frac{2\omega_0 \Gamma_0 e^{-\Gamma_0 T}}{c^3 \epsilon_0^2 \hbar} \boldsymbol{\mu}_b \wedge \boldsymbol{\nabla} \wedge \mathrm{Im}\, \mathbb{G}(k_0 R) \cdot \boldsymbol{\mu}_A \int_0^\infty \frac{dq}{\pi} \frac{(q^2 - k_0^2) q^2 \boldsymbol{\mu}_A \cdot \mathbb{G}(iqR) \cdot \boldsymbol{\mu}_b}{\left(q^2 + k_0^2\right)^2} \Bigg\}. \end{aligned} \tag{B2}$$

[1] J. B. Pendry, J. Phys.: Condens. Matter **9**, 10301 (1997).
[2] F. Intravaia, V. E. Mkrtchian, S. Y. Buhmann, S. Scheel, D. A. R. Dalvit, and C. Henkel, J. Phys.: Condens. Matter **27**, 214020 (2015).
[3] M. Donaire and A. Lambrecht, Phys. Rev. A **93**, 022701 (2016).
[4] F. Verstraete, M. M. Wolf, and J. I. Cirac, Nat. Phys. **5**, 633 (2009).
[5] S. Diehl, W. Yi, A. J. Daley, and P. Zoller, Phys. Rev. Lett. **105**, 227001 (2010).
[6] M. Lemeshko and H. Weimer, Nat. Commun. **4**, 2230 (2013).
[7] J. J. Sakurai, *Advanced Quantum Mechanics*, (Addison-Wesley, Boston, 1967).
[8] M. E. Peskin and D. V. Schroeder, *An Introduction to Quantum Field Theory*, (Westview, Chicago, 1995).
[9] C. Cohen-Tannoudji, J. Dupont-Roc, and G. Grynberg, *Photons and Atoms. Introduction to Quantum Electrodynamics* (WILEY-VCH, Weinheim, 2004).
[10] F. London, Z. Phys. **63**, 245 (1930); H. B. G. Casimir and D. Polder, Phys. Rev. **73**, 360 (1948).
[11] J. M. Wylie and J. E. Sipe, Phys. Rev. A **30**, 1185 (1984); **32**, 2030 (1985).
[12] P. W. Milonni, *The Quantum Vacuum* (Academic, San Diego, 1994).
[13] K. A. Milton, *The Casimir Effect: Physical Manifestations of Zero-point Energy* (World Scientific, Singapore, 2001).
[14] S. Y. Buhmann, *Dispersion Forces I: Macroscopic Quantum Electrodynamics and Ground-Sate Casimir, Casimir-Polder and van der Waals Forces* (Springer, Berlin, 2012).
[15] S. Y. Buhmann, *Dispersion Forces II: Many-Body Effects, Excited Atoms, Finite Temperature and Quantum Friction* (Springer, Berlin, 2012).
[16] D. P. Craig and T. Thirunamachandran, *Molecular Quantum Electrodynamics* (Dover, New York, 1998).
[17] S. Scheel and S. Y. Buhmann, Acta Phys. Slovaca **58**, 675 (2008).
[18] L. Rizzuto, R. Passante, and F. Persico, Phys. Rev. A **70**, 012107 (2004).
[19] P. R. Berman, Phys. Rev. A **91**, 042127 (2015).
[20] M. Donaire, R. Guérout, and A. Lambrecht, Phys. Rev. Lett. **115**, 033201 (2015).
[21] P. W. Milonni and S. M. H. Rafsanjani, Phys. Rev. A **92**, 062711 (2015).
[22] P. Barcellona, R. Passante, L. Rizzuto, and S. Y. Buhmann, Phys. Rev. A **94**, 012705 (2016).
[23] Y. Sherkunov, Phys. Rev. A **72**, 052703 (2005).
[24] Y. Sherkunov, Phys. Rev. A **97**, 032512 (2018).
[25] R. O. Behunin and B. L. Hu, Phys. Rev. A **82**, 022507 (2010).
[26] M. Donaire, Phys. Rev. A **93**, 052706 (2016).
[27] M. Donaire, Phys. Rev. A **94**, 062701 (2016).
[28] J. Sánchez-Cánovas and M. Donaire, Phys. Rev. A **104**, 052814 (2021).

[29] O. Dippel, P. Schmelcher, and L. S. Cederbaum, Phys. Rev. A **49**, 4415 (1994).

[30] B. A. van Tiggelen, S. Kawka, and G. L. J. A. Rikken, Eur. Phys. J. D **66**, 272 (2012).

[31] S. Kawka, Moment de Casimir: Effet du vide quantique sur l'impulsion d'un milieu bi-anisotrope, Ph.D. thesis, Laboratoire de physique et modélisation des milieux condensés; Available online at https://tel.archives-ouvertes.fr/tel-00576211.

[32] C. Baxter, M. Babiker, and R. Loudon, Phys. Rev. A **47**, 1278 (1993).

[33] V. E. Lembessis, M. Babiker, C. Baxter, and R. Loudon, Phys. Rev. A **48**, 1594 (1993).

[34] We neglect a Röntgen's term in Eq. (2) $[\mathbf{P}_{A,B}\cdot[\mathbf{d}_{A,B}\wedge\mathbf{B}(\mathbf{R}_{A,B})]+[\mathbf{d}_{A,B}\wedge\mathbf{B}(\mathbf{R}_{A,B})]\cdot\mathbf{P}_{A,B}]/2m_{A,B}$ for its contributions to Eq. (1) as well as to any time-dependent expectation value are of orders $\dot{R}_{A,B}/c$ and $\mathbf{d}_{A,B}\cdot\mathbf{E}(\mathbf{R}_{A,B})/m_{A,B}$ smaller than the contributions of the term in Eq. (2) [3].

[35] M. Donaire, B. A. van Tiggelen, and G. L. J. A. Rikken, J. Phys.: Condens. Matter **27**, 214002 (2015).

[36] M. Donaire, B. A. van Tiggelen and G. L. J. A. Rikken, Phys. Rev. Lett. **111**, 143602 (2013).

[37] S. Fuchs and S. Y. Buhmann, Europhys. Lett. **124**, 34003 (2018).

[38] K. Sinha, B. P. Venkatesh, and P. Meystre, Phys. Rev. Lett. **121**, 183605 (2018).

[39] J. M. Raimond, G. Vitrant, and S. Haroche, J. Phys. B: At. Mol. Phys. **14**, L655 (1981).

[40] A. Reinhard, T. C. Liebisch, B. Knuffman, and G. Raithel, Phys. Rev. A **75**, 032712 (2007).

[41] A. Paris-Mandoki, H. Gorniaczyk, C. Tresp, I. Mirgorodskiy, and S. Hofferberth, J. Phys. B: At., Mol. Opt. Phys. **49**, 164001 (2016).

[42] S. Weber *et al.*, J. Phys. B: At., Mol. Opt. Phys. **50**, 133001 (2017).

[43] S. Ribeiro, S. Y. Buhmann, T. Stielow, and S. Scheel, Europhys. Lett. **110**, 51003 (2015).

[44] E. Urban, T. A. Johnson, T. Henage, L. Isenhower, D. D. Yavuz, T. G. Walker, and M. Saffman, Nat. Phys. **5**, 110 (2009); A. Gaëtan, Y. Miroshnychenko, T. Wilk, A. Chotia, M. Viteau, D. Comparat, P. Pillet, A. Browaeys, and P. Grangier, *ibid.* **5**, 115 (2009); T. Wilk, A. Gaëtan, C. Evellin, J. Wolters, Y. Miroshnychenko, P. Grangier, and A. Browaeys, Phys. Rev. Lett. **104**, 010502 (2010).

[45] L. Béguin, A. Vernier, R. Chicireanu, T. Lahaye, and A. Browaeys, Phys. Rev. Lett. **110**, 263201 (2013).